ACS Energy LETTERS

Cite This: ACS Energy Lett. 2019, 4, 2168−2180

http://pubs.acs.org/journal/aelccp

PERSPECTIVE

Engineered Enzymes and Bioinspired Catalysts for Energy Conversion

Jennifer M. Le and Kara L. Bren*

Department of Chemistry, University of Rochester, Rochester, New York 14627, United States

ABSTRACT: **Metalloenzymes play critical roles in the environment by catalyzing redox reactions in biogeochemical cycles. The elucidation of structure−function relationships in these biocatalysts has provided a foundation for the development of bioinspired catalysts for fuel production and small-molecule activation. In this Perspective, we highlight developments in engineered biomolecular and bioinspired catalysts for the reduction of H^+, O_2, and CO_2 and for the oxidation of H_2 and H_2O. The roles of proton transfers and second-sphere interactions in particular are highlighted.**

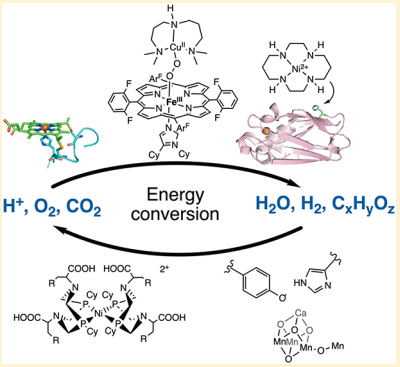

Metalloenzymes catalyze a number of energy-relevant multielectron, multiproton reactions (Table 1). The key bond-making and bond-breaking steps typically occur at one or more active-site metal ions, but the protein matrix is critical for providing second-sphere interactions and pathways dedicated to transferring small-molecule substrates and products, as well as electrons and protons. In many cases, redox reactions carried out by metalloenzymes use proton-coupled electron-transfer (PCET) steps, circumventing high-energy intermediates.[1−3] Some limitations of metalloenzymes hindering their use in energy conversion systems are that they may be prone to degradation outside of their native environment and that they have a low density of active sites. However, introducing key active-site features of metalloenzymes in engineered biomolecular or bioinspired synthetic catalysts may yield systems with enhanced efficiency and activity. Furthermore, mimicking the function of metalloenzymes is a route to understanding structure−function relationships and mechanisms of nature's enzymes.

> The protein matrix is critical for providing second-sphere interactions and pathways dedicated to transferring small-molecule substrates and products, as well as electrons and protons.

In this Perspective, we highlight developments in the preparation and investigation of biomolecular and bioinspired catalysts for energy-relevant multiproton, multielectron reactions. The literature in this area is vast, and this Perspective is not meant to be a comprehensive review. Rather, we select illustrative examples of advances relevant to catalysis for each of the reactions shown in Table 1. For each reaction, we focus on two different approaches. One is the modification or preparation of a biomolecule (typically a protein) that mimics the activity of the natural enzyme. The second is the preparation of a synthetic small-molecule complex that incorporates features proposed to be important for the activity of the enzyme, such as second-sphere interactions or a proton-shuttle site. Finally, we provide remarks on the state of the field and areas for future development.

Table 1. Examples of Metalloenzymes That Catalyze Multielectron and Multiproton Reactions

enzyme	reaction catalyzed
hydrogenase	H^+ reduction/H_2 oxidation
	$2H^+ + 2e^- \rightleftharpoons H_2$
cytochrome *c* oxidase	O_2 reduction
	$O_2 + 4e^- + 4H^+ \rightarrow 2H_2O$
photosystem II	H_2O oxidation
	$2H_2O \rightarrow O_2 + 4e^- + 4H^+$
carbon monoxide dehydrogenase	CO_2 reduction
	$CO_2 + 2H^+ + 2e^- \rightarrow CO + H_2O$

H^+ Reduction/H_2 Oxidation. Hydrogenases catalyze the hydrogen evolution reaction, in which protons (H^+) are reduced to hydrogen (H_2) (Scheme 1). They also catalyze H_2 oxidation, although the bias toward oxidation or reduction varies among enzymes.[4−6] Hydrogenases are remarkable for catalyzing these reactions rapidly at low overpotential,[7,8] a

Received: June 18, 2019
Accepted: August 5, 2019
Published: August 5, 2019

DOI: 10.1021/acsenergylett.9b01308
ACS Energy Lett. 2019, 4, 2168−2180

Scheme 1

$$H_2O \rightarrow \tfrac{1}{2}O_2 + 2H^+ + 2e^- \text{ (water oxidation)}$$
$$2H^+ + 2e^- \rightarrow H_2 \text{ (proton reduction)}$$

thermodynamic parameter that describes the additional potential beyond the thermodynamic potential required to drive a reaction at a specific rate.[9] The facile and efficient interconversion of H^+/H_2 by hydrogenases makes them candidates for H_2 production and fuel cell catalysts. However, these enzymes lack the needed robustness for such applications, are typically oxygen-sensitive[4] (although successful efforts to engineer oxygen-tolerant hydrogenases are well underway[10,11]), and have low active-site densities. An alternative to using hydrogenases for H_2 production/oxidation is conferring hydrogenase activity on a metalloprotein through metal substitution or by incorporating a cofactor or synthetic catalyst into a protein scaffold. Furthermore, synthetic catalysts mimicking nature's catalysts by incorporating second-sphere interactions and/or by installing proton relays near the active site are being actively pursued.[12]

Engineered Protein Catalysts for H^+ Reduction. The effects that a protein matrix can confer on catalyst overpotential and robustness are illustrated by studies of a series of catalysts consisting of a cobalt porphyrin covalently bound to one or two peptides. The first and simplest of these is CoMP11-Ac,[13] which is prepared by cobalt substitution for iron in the cytochrome *c*-derived heme-peptide complex known as microperoxidase-11 (MP11), followed by acetylation of free amines.[14] CoMP11-Ac consists of cobalt protoporphyrin IX covalently attached to an 11-amino acid chain through a Cys-X_{aa}-X_{aa}-Cys-His motif providing an axial histidine ligand on the proximal side of the porphyrin (Figure 1a). Unlike many porphyrin-based catalysts,[15−17] CoMP11-Ac functions in water. CoMP11-Ac operates at an overpotential of 690 mV (using the half-wave potential) at pH 7.0, and its electrocatalytic activity drops significantly after only 15 min of controlled potential electrolysis (CPE). Nevertheless, its high activity contributes to its good turnover number (TON) of 25 000.[13]

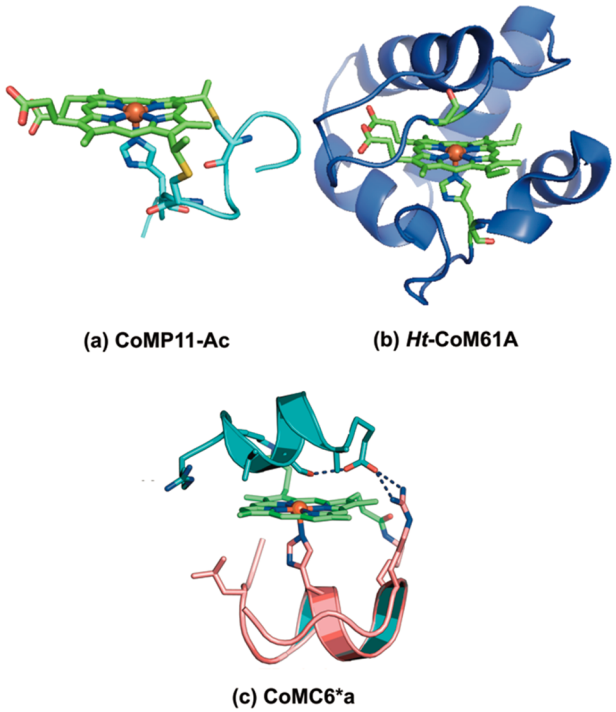

Figure 1. (a) CoMP11-Ac (PDB ID: 1CRC). (b) *Ht*-CoM61A (PDB ID: 1AYG). (c) Model of CoMC6*a.

The short lifetime of CoMP11-Ac stimulated the production of other biocatalysts with a similar cobalt porphyrin active site, but with polypeptides on both sides of the porphyrin, which were predicted to be more robust. One is a cobalt-substituted mutant of *Hydrogenobacter thermophilus* cytochrome c_{552} (*Ht*-CoM61A, Figure 1b).[18] This catalyst is indeed more robust, lasting for ∼5 h of CPE and giving a 10-fold higher TON of 270 000. However, the 730 mV overpotential for *Ht*-CoM61A (using the half-wave potential) at pH 7.0 is higher than that of CoMP11-Ac. This problem was addressed in the third of these cobalt-porphyrin-based catalysts, a synthetic cobalt-heme miniprotein (CoMC6*a, Figure 1c). Investigations of this protein revealed that enhancing peptide folding in this case *lowers* overpotential by up to 90 mV from 610 mV to 520 mV (using the half-wave potential). Catalyst longevity is also enhanced relative to that of CoMP11-Ac to 1.3 h in CPE, giving a TON of 230 000.[19] These examples demonstrate that a peptide scaffold can impact robustness and efficiency of a cobalt-porphyrin active site for H_2 evolution.[19]

Artificial hydrogenases also have been produced by incorporating a synthetic small-molecule catalyst into a polypeptide scaffold, with goals of enhancing water solubility and stability and lowering overpotential. An early example is a demonstration that attachment of a peptide bearing a photoactive Ru complex to a diiron model of the [FeFe]-hydrogenase active site yields a system that is active for light-driven H_2 production from water in the presence of a photosensitizer and electron donor, yielding a TON ≈ 9. Notably, the same system with the photosensitizer freely diffusing shows no activity.[20] The activity enhancement is attributed to improved electron transfer in the integrated system, mimicking intramolecular electron delivery seen in nature. Another example incorporates "cobaloximes" (Figure 2), which are well-studied H_2-evolution catalysts typically employed in organic solvents or mixtures with water.[21] Two cobaloxime derivatives with difluoroboronyl-(**1**) and proton-bridged (**2**) glyoxime ligands were incorporated into sperm-whale myoglobin, yielding *Sw*Mb·**1** and *Sw*Mb·**2**, respectively.[22] In studies via cyclic voltammetry (CV) in water at pH 7, the protein environment in *Sw*Mb·**1** shifts the Co(II/I) potential 100 mV more negative than the free complex **1**, providing insight into factors that control the potential of this catalytically relevant redox couple. In photocatalytic experiments pairing these catalysts with photosensitizers and electron donors, the highest TONs achieved for *Sw*Mb-**1** and *Sw*Mb-**2** are 3.8 and 5, respectively. Although the TON values are low, this work demonstrates the successful introduction of synthetic catalysts into a protein scaffold to yield a water-compatible system with H_2-evolution activity.

An in-depth investigation of protein secondary-sphere effects on H_2 evolution by a synthetic catalyst is reported for Co-protoporphyrin IX encapsulated in myoglobin (CoMyo).[23] In a photocatalytic system, CoMyo displays enhancement in TON by a factor of up to 4 relative to free Co-protoporphyrin IX (studied in acetonitrile), again demonstrating longevity enhancement by placing a catalyst in a polypeptide matrix. Furthermore, active-site mutations were found to impact TON

DOI: 10.1021/acsenergylett.9b01308
ACS Energy Lett. 2019, 4, 2168−2180

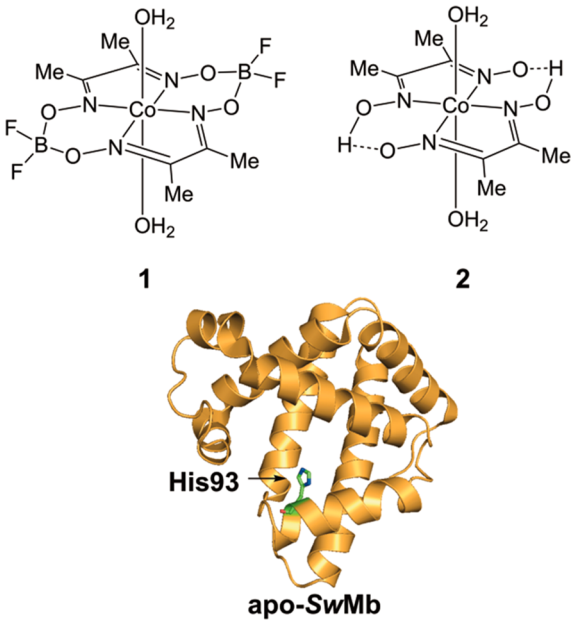

Figure 2. Structures of 1 and 2 and model of apo-*Sw*Mb showing H93 of the binding pocket (PDB ID: IUFJ).

and pH dependence of catalysis, illustrating the importance of the detailed active-site structure.[23] A related study of polypeptide effects on catalyst activity takes advantage of the high affinity of the biotin ligand for streptavidin, incorporating biotinylated aminopyridine cobalt complexes in streptavidin.[24] Similar to what was observed for CoMC6*a, this construct has a lowered overpotential (by 100 mV) relative to the catalyst without protein. Molecular dynamics simulations reveal that polar residues positioned near the active site may assist with proton transfer to enhance activity.[24] This study is a rare example of successful enhancement of synthetic catalyst efficiency by incorporation into a polypeptide.

Bioinspired Synthetic Catalysts for H^+ Reduction or H_2 Oxidation. The study of coordination complexes that catalyze H^+ reduction to H_2 goes back many decades.[25] Early studies predated our current understanding of hydrogenase enzyme structure and function. Now, chemists successfully draw on our knowledge of enzyme structure and mechanism in catalyst design. A particularly successful example is seen in synthetic nickel catalysts of the $[Ni(P_2^RN_2^{R'})_2]^{2+}$-type (Figure 3a). These complexes have proton shuttles in the form of pendant amines that participate in the formation and/or cleavage of the H_2 bond,[26−28] modeling the role of the azadithiolate bridging ligand in [FeFe]-hydrogenase.[29,30] Furthermore, appending amino acids and peptides to the catalyst confers water solubility and has a significant influence on H_2 production and/or oxidation activity. In these systems, the R′ group is a single amino acid or dipeptide, and the R group is a cyclohexyl group. Derivatives that contain a single aspartic acid (Asp) or arginine (Arg) in the R′ position catalyze reversible H_2 oxidation in water. The Asp derivative performs reversible H_2 oxidation at pH 0 with an overpotential of 150 mV (for the oxidation reaction using the half-wave potential) and turnover frequency (TOF) of 10 s^{-1}.[31] Interestingly, the Arg derivative catalyzes reversible H_2 oxidation in water over a broader pH range (0−6) at a similarly low overpotential of 180 mV, reaching a maximum TOF of 210 s^{-1} at pH 0.1.[32] These studies are excellent examples of taking simple building blocks from nature such as a pendant amino group and amino acids, installing them on a synthetic catalyst, and varying them to gain insight into effects of the secondary coordination sphere on catalytic activity and efficiency.

> Now, chemists successfully draw on our knowledge of enzyme structure and mechanism in catalyst design.

While the above system models the role of the [FeFe]-hydrogenase pendant amine ligand and proton relays, others more closely resemble the full diiron cofactor. A recent example for selective H_2 generation in the presence of O_2 includes substituted arenes attached to the bridgehead nitrogen in the sulfur-to-sulfur linker modeled after the azadithiolate bridging ligand in [FeFe]-hydrogenaeses (Figure 3b).[33] Electrochemical studies of the *ortho*-substituted derivatives catalyzing H_2 generation in pH 5.5 water reveal low overpotentials of 180−190 mV (using the onset potential) and high TONs > 1 000 000. The high activity for H_2 generation and tolerance to O_2 are attributed to control of the orientation of bridgehead nitrogen lone pair and its enhanced ability to act as a proton relay.

There also are H_2-evolution catalysts featuring second-sphere interactions and/or proton shuttles that do not mimic the hydrogenase active site structure. The cobalt complex of the Gly-Gly-His tripeptide (CoGGH) is an electrocatalyst that features a peptide moiety, but in this case as a ligand to the metal ion (Figure 3c).[34] This complex is a model of the amino-terminal copper- and nickel-binding (ATCUN) motif found in a number of copper-binding proteins.[35] CoGGH functions in water to produce H_2 in the presence of oxygen at an overpotential of 600 mV (using the half-wave potential) at pH 8.0. The activity of CoGGH lasts up to 2.5 h in CPE, giving a modest TON of 275. CoGGH represents a class of H_2-evolution catalyst that is straightforward to synthesize and that features an amine positioned near the cobalt that may function in proton-coupled electron transfer (PCET) during catalysis.

Other examples where PCET is observed in a synthetic catalyst with a built-in proton relay are the "hangman porphyrins" that feature a carboxylic acid on a xanthene ring positioned over a metal ion (Figure 3d). Mechanistic studies of H_2 production by the hangman porphyrin catalysts have contributed much insight into mechanism involving the porphyrin ligand.[36−38] These studies reveal the unexpected reactivity from the porphyrin to form an organo hydride and identify divergent mechanistic pathways in the presence of weak and strong acids. For example, in the nickel analogue, theoretical analyses reveal that under weak acid conditions, the reduction of Ni(II) to Ni(I) is followed by a reduction of the porphyrin. This leads to an intramolecular proton transfer from the carboxylic acid to the *meso* carbon, accompanied by an electron transfer from the Ni(I) center to the porphyrin. Spectroelectrochemical studies further corroborate the formation of a protonated porphyrin intermediate. Under strong acid conditions, the Ni(I) species interacts directly with acid, and a PCET step occurs where proton transfer from the acid and electron transfer from the Ni(I) species yields the protonated *meso* carbon.[37] Not only does this well-characterized system demonstrate that the porphyrin ligand can transfer both electrons and protons in catalysis, but it uncovers

DOI: 10.1021/acsenergylett.9b01308
ACS Energy Lett. 2019, 4, 2168−2180

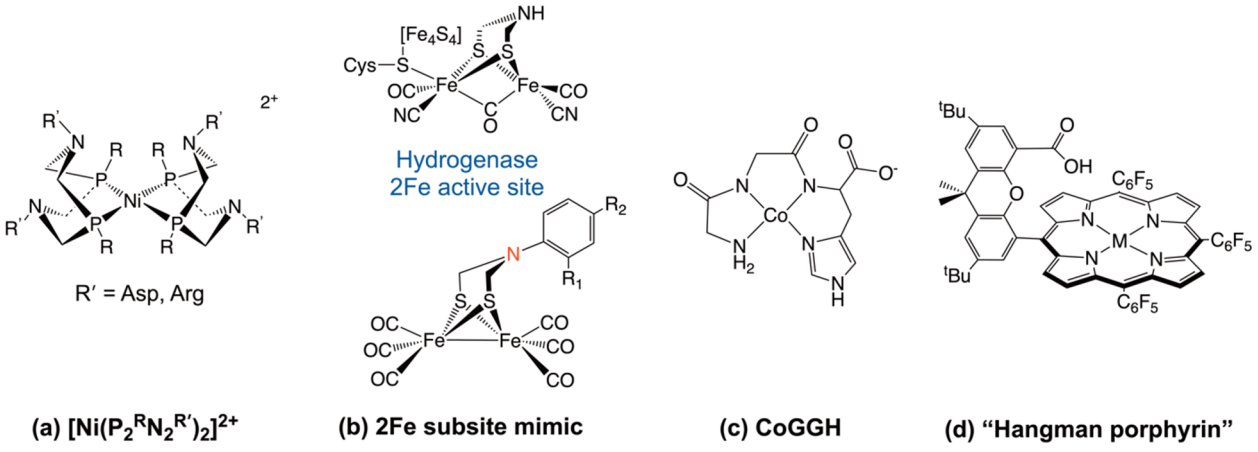

Figure 3. Drawings of (a) the $[Ni(P_2^RN_2^{R'})_2]^{2+}$ catalyst where R = cyclohexyl and R′ = Asp or Arg; (b) the representative 2Fe subsite mimic from ref 33 (bottom) and the 2Fe active site in [FeFe]-hydrogenase (top); (c) CoGGH; (d) and the "hangman porphyrin," where "M" is the metal.

the surprising reactivity of a C−H intermediate that is involved in H_2-evolution steps usually invoked for the metal-hydride.[39]

Progress and Challenges in H_2 Production and Oxidation. A significant advance in the field of H_2-evolution catalyst development has been the demonstration that introducing proton-transfer pathways can yield more efficient catalysts. These results also enhance our broad understanding of natural enzyme catalysis. Another advance has been the development of synthetic H_2-evolution catalysts that function in 100% water. As water is our most abundant and sustainable proton source and a desirable solvent, this has been a valuable direction.

Despite the great progress in the H_2-evolution catalysis field, there remain exciting opportunities for future development. There has been much more progress in H_2 production catalysis than H_2 oxidation catalysis, and catalysts that perform the reversible reaction are even more rare. Progress would be supported by further mechanistic investigations of catalyst−H_2 interaction and H_2 cleavage in the existing systems. In addition, investigations of factors limiting activity and leading to catalyst deactivation would help researchers design more robust systems. Broadly speaking, our understanding of mechanism requires further development, especially for systems that function in water. Ultimately, integrating H_2-evolution catalysts with catalysts for water oxidation is needed to yield systems for full water splitting, and this task brings with it additional challenges of catalyst compatibility and the need to transfer electrons and protons between the oxidation and reduction sides of the reaction.

O_2 Reduction. Oxygen reduction is fundamental to aerobic respiration and is a key reaction in some fuel cells and in metal−air batteries. The desired reaction in fuel cells is the $4e^-/4H^+$ reduction of dioxygen (O_2) to water (H_2O) (Table 1), which is challenging for a number of reasons. For one, there is a high thermodynamic barrier to the initial $1e^-$ reduction step to form superoxide. Second, the four-electron reaction tends to have slow overall kinetics.[40,41] Finally, partial reduction products are readily formed and can yield deleterious side reactions and catalyst degradation (Scheme 2).[42] The catalysts for O_2 reduction in current fuel cell technologies are mainly platinum-based,[43] which is not sustainable. In contrast, the enzyme cytochrome *c* oxidase (C*c*O) catalyzes O_2 reduction selectively to H_2O with earth-abundant metals iron and copper.[44,45] C*c*O accepts electrons

Scheme 2

$$O_2 + e^- \rightarrow O_2^{\bullet -} \text{ (Superoxide)}$$
$$O_2 + 2e^- + 2H^+ \rightarrow H_2O_2 \text{ (Peroxide)}$$
$$O_2 + 3e^- + 3H^+ + \rightarrow OH^{\bullet} + H_2O \text{ (Hydroxyl radical)}$$

from cytochrome *c* through a binuclear copper center and transfers them to the heme a_3-Cu_B active site (Figure 4a),[44,46]

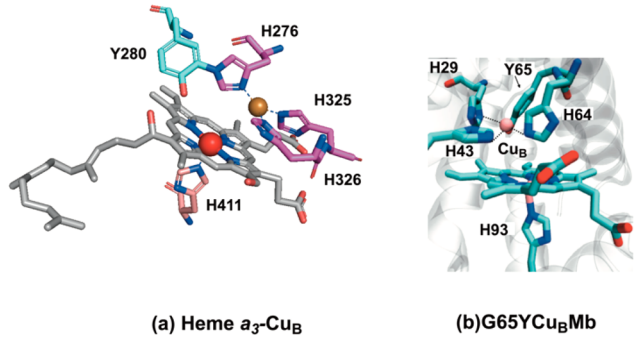

Figure 4. (a) Heme a_3-Cu_B site in cytochrome *c* oxidase (C*c*O, PDB ID: 3EHB). Cu is shown as the brown sphere, and Fe is shown as the red sphere. (b) Model of G65YCu_BMb. Reprinted with permission from ref 50. Copyright 2015 Springer Nature.

where second-sphere interactions play a role in controlling O_2 binding and activation for reduction to H_2O.[47] Akin to C*c*O, many bioinspired catalysts feature a second metal site and second-sphere interactions to activate the O−O bond, facilitate multielectron/multiproton chemistry, and/or produce H_2O selectively.[48]

Engineered Proteins for O_2 Reduction. Myoglobin, a robust and well-characterized O_2-binding heme protein, is an ideal template for modeling activity of heme enzymes.[48,49] To mimic the C*c*O heme a_3-Cu_B O_2 reduction site (Figure 4a) within a myoglobin scaffold, the distal heme pocket residues leucine (L29) and phenylalanine (F43) were both mutated to histidine to yield a His_3 metal-binding site near the heme that includes the native H64 (protein is termed Cu_BMb).[50] A glycine-to-tyrosine (G65Y) mutation was also included (G65YCu_BMb, Figure 4b) to structurally mimic the C*c*O active-site tyrosine (Y280; Figure 4a). Taking advantage of the solvent-exposed

DOI: 10.1021/acsenergylett.9b01308
ACS Energy Lett. 2019, 4, 2168−2180

propionate groups of the native heme cofactor, the protein was reconstituted with a "hemin-yne" group in place of the native heme. The hemin-yne enabled functionalization of G65YCu$_B$Mb onto an electrode, allowing the authors to engineer a molecular wire from an electrode to the active site and facilitate characterization using rotating disc electrode (RDE) and rotating ring disc electrode (RRDE) methods. This approach revealed that O_2 is fully reduced by 4e$^-$ to H_2O by G65YCu$_B$Mb with a TON of 10 000 and TOF of 5 000 s^{-1} at pH 7.0. Notably, only 6% of O_2 is converted to partially reduced O_2 species (Scheme 2). This study demonstrates that the introduction of a small number of mutations into an O_2-carrying heme protein can yield a catalyst for the full reduction of O_2. It also enhances our understanding of the role of the Cu$_B$ ion in C*c*O.

A subsequent study of a Mb derivative with a metal-binding site installed near the heme (Fe$_B$Mb, modeling NO reductase) focused on the role of the "Fe$_B$-site" metal ion in O_2 activation and electron transfer by evaluating O_2 reduction activity when Zn(II), Cu(I), or Fe(II) is in the Fe$_B$ site.[51] The zinc variant reduces 57% of O_2 to H_2O, whereas the iron and copper variants give near quantitative reduction to H_2O. Furthermore, the iron and copper variants have 11-fold and 30-fold higher H_2O production rates than the zinc variant, respectively. The authors propose that the higher potential for the Cu(II/I) couple (387 mV, vs 259 mV for Fe(III/II)) may drive faster electron transfer to support the faster H_2O production rate observed for the copper variant relative to the iron variant. Supporting spectroscopic and density functional theory (DFT) analyses support the proposal that O_2 binds to and oxidizes heme and Fe or Cu. It is evident that having a redox-active metal in the Fe$_B$ site facilitates the full four-electron reduction of O_2. These studies on myoglobin variants showcase how the protein modeling approach yields detailed information on the functional roles of key features in the active site of a complex enzyme like C*c*O.

These studies on myoglobin variants showcase how the protein modeling approach yields detailed information on the functional roles of key features in the active site of a complex enzyme like C*c*O.

Subtle differences in second-sphere interactions can determine whether a metalloprotein binds O_2 reversibly or activates O_2 for further chemistry. It has been noted that O_2-carrying heme proteins have at least one H-bond interacting with the proximal oxygen atom (O_p) in O_2 in the heme Fe−O_2 adduct (Figure 5a),[52] whereas O_2-activating enzymes such as peroxidases, oxidases, and cytochrome P450s involve one H-bond with the distal oxygen atom (O_d).[53−56] H-bonding to the O_d atom is proposed to facilitate substrate C−H activation.[57,58] This hypothesis was tested by incorporating a biotinylated-Cu(II) complex into streptavidin (Sav).[59] Crystallographic data show that an aqua ligand from Cu(II) is H-bonded to one of the structural water molecules (O1) that is stabilized through H-bonding to a serine residue (S112) in Sav. Treating this complex with hydrogen peroxide generates a Cu(II)-OOH adduct that is stabilized by an H-bond from an arginine residue (N49) to the O_d atom of Cu(II)-OOH as well as another H-bond from the O1 to the O_p atom (Figure 5b). Interestingly, a Sav S112A mutant removes the occupancy of O1, thereby breaking the H-bonding network between the O_p atom of Cu(II)-OOH and S112, leaving one H-bond between the O_d atom and N49. This variant catalyzes the oxidation of 4-chlorobenzylamine, whereas the variant with S112 H-bonded to the O_p atom does not. This result supports the hypothesis that H-bonding with O_d promotes O_2 activation. Although this system does not perform the O_2 reduction reaction, it elegantly demonstrates how an intimate network of H-bonding and specific second-sphere interactions impact O_2 activation.

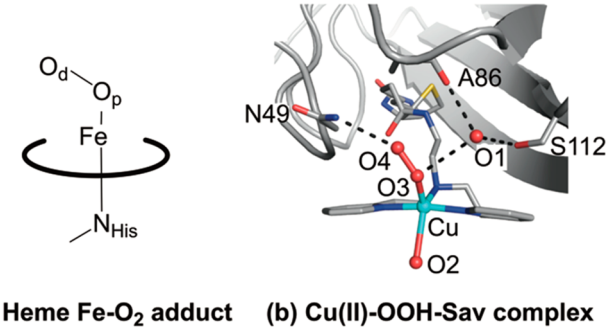

Figure 5. (a) Representation of the proximal (O_p) and distal (O_d) oxygens of the heme Fe−O_2 adduct. (b) Cu(II)-OOH-Sav complex. O4 and O3 represent the O_d and O_p oxygen atoms, respectively. O1 represents the structural water molecule H-bonded to S112. Panel b is reprinted from ref 59. Copyright 2017 American Chemical Society.

Bioinspired Synthetic Systems for O_2 Reduction. Inspired by nature's use of iron porphyrins for oxygen activation, a number of iron porphyrin complexes incorporating features inspired by the C*c*O heme pocket have been successfully employed for O_2 reduction catalysis.[42] One such system is notable for its excellent performance in terms of high selectivity (>90%) and high rate (>10^7 M^{-1} s^{-1}) for O_2 reduction to H_2O when adsorbed on electrode surfaces.[60] These models incorporate basic distal moieties proposed to activate the O−O bond for cleavage and promote proton transfer to the distal oxygen of Fe-bound O_2, inspired by the proton-transfer pathways and H-bonding groups in C*c*O and related enzymes. Notably, by varying the basicity of the pendant group as well as the number of donors, the researchers demonstrated how both factors tune reactivity. The availability of crystal structures of O_2 adducts of the models is particularly valuable.

A feature characteristic of C*c*O is the covalent His-Tyr cross-link involving one of the histidine ligands bound to Cu$_B$. This motif is proposed to play a role in donating a proton and an electron for O_2 reduction to H_2O.[61] The hypothesis is that a heme-peroxo-copper intermediate is cleaved by a net H-atom transfer from tyrosine (Figure 6a).[61,62] However, there is not strong evidence for either the peroxo intermediate or the involvement of the tyrosine in the net H-atom transfer for O−O bond cleavage in C*c*O.[62−64] To probe the role of H-atom transfer from phenols in O_2 activation, a biomimetic heme-peroxo-copper complex, {[DCHIm)(F_8)-Fe^{III}]−(O_2^{2-})−[Cu^{II}(AN)]}$^+$(**1**, Figure 6b) was prepared.[63] This complex is reactive as an H-atom-acceptor in the presence of exogenous 4-OMe-PhOH to generate a phenoxyl radical, providing support that a heme-peroxo-copper intermediate may exist before the O−O bond is cleaved to generate the Fe^{IV}=O/Cu^{II}−OH/Y* species (Figure 6a). The choice of an exogenous phenol to

DOI: 10.1021/acsenergylett.9b01308
ACS Energy Lett. 2019, 4, 2168−2180

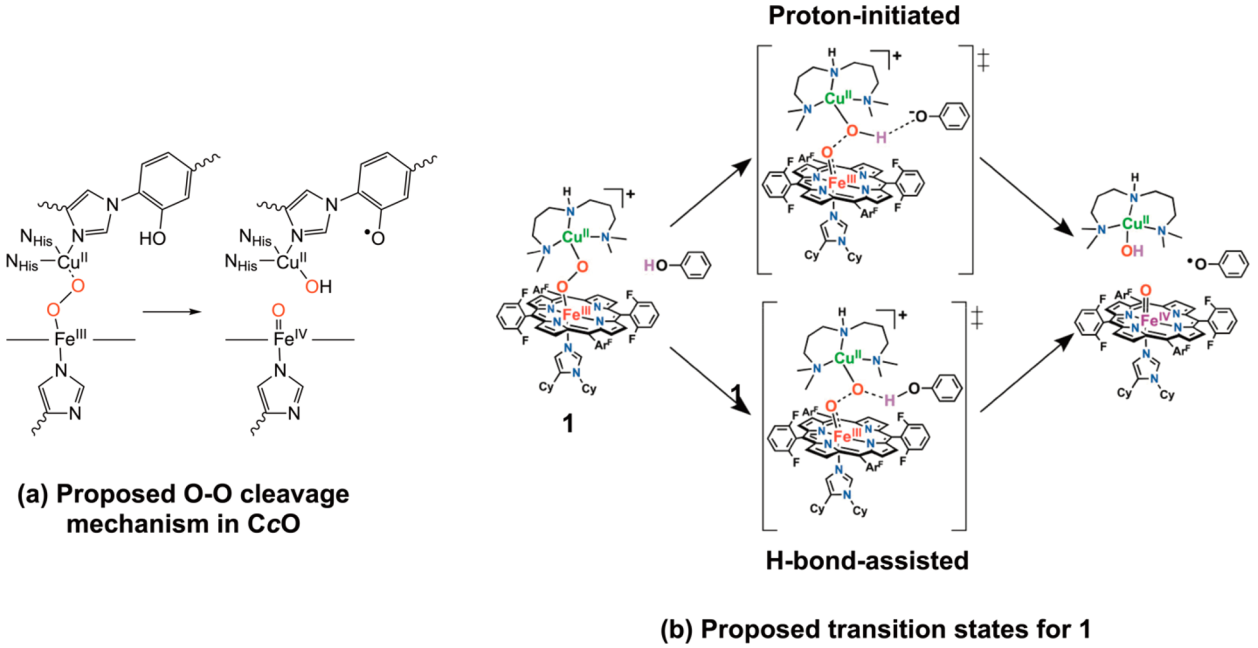

Figure 6. (a) Proposed O−O cleavage in CcO via a net H-atom transfer from tyrosine to a peroxo intermediate. (b) Proposed transition states for O−O cleavage for the biomimetic heme-peroxo-copper complex. Reprinted from ref 63. Copyright 2017 American Chemical Society.

provide a H^+ and an e^- provided a well-defined system for detailed DFT calculations. Two different transition states are proposed, described as "proton-initiated" and "H-bond-assisted" (Figure 6b), and in both cases, the authors suggest that O−O bond cleavage in C*c*O is likely to be facilitated by the tyrosine. Kinetic isotope effect studies reveal that the H-bond-assisted pathway occurs rather than the proton-initiated pathway. This elegant study reveals in detail ways in which an active-site tyrosine or related group may facilitate O_2 reduction.

Some systems for probing roles of second-sphere interactions in O_2 reduction do not resemble enzyme active sites but nevertheless provide valuable insights into factors important in biocatalyst activity. One example is a Mn(II) catalyst for O_2 reduction to H_2O featuring a tripodal ligand with two urea groups and one carboxyamidopyridyl group forming an N_4O Mn coordination site ($[Mn(II)H_2$ bupa$]^-$) (Figure 7).[65] This system is notable for illustrating how the relative acidities of second-sphere H-bond donors play a role in reactivity.[66] The authors propose that the less acidic urea groups (pK_a values >27 in DMSO) provide H-bonds to stabilize O_2 adducts, while the more acidic carboxyamido group (pK_a = 22 in DMSO) donates a proton to facilitate O−O bond cleavage. The carboxyamido group enhances the release of the first equivalent of water by proton donation to one of the hydroxo ligands. In contrast, no water is formed in the case where all three ligands of the complex are urea ligands. This study demonstrates that the relative acidities of groups in the secondary coordination sphere can be tuned to enhance both O_2 binding and H_2O product release.

Progress and Challenges in O_2 Reduction. Significant advances have been made toward understanding how second-sphere interactions with O_2 and related species impact O_2-reduction pathways. Toward elucidating structure−activity relationships in the complex enzyme C*c*O, artificial metalloenzyme catalysts and bioinspired synthetic catalysts that incorporate key

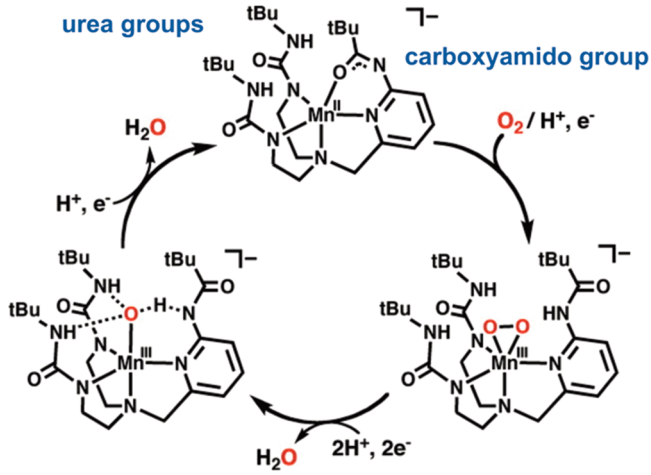

Figure 7. Proposed catalytic cycle for O_2 reduction to H_2O by $[Mn(II)H_2$ bupa$]^-$. Reprinted from ref 65. Copyright 2011 American Chemical Society.

features such as a second metal site, an H-bonding network, proton donors, and redox-active organic moieties have advanced our understanding of the requirements for O_2 activation and O−O bond cleavage. An ongoing challenge in O_2 reduction catalysis is the formation of partially reduced O_2 intermediates (Scheme 2), reducing efficiency and initiating side reactions, although systems have now been developed that limit the formation of partial O_2 reduction products. In particular, managing protons and tuning second-sphere interactions are critical to meeting this goal. Alternatively, including systems for the removal or diversion of partially reduced O_2 species may be considered, but these strategies decrease efficiency and add to the complexity of the overall system. The development of O_2-reduction catalysts using abundant elements with robustness and efficiency sufficient to substitute for platinum in fuel cells is a challenging ultimate

DOI: 10.1021/acsenergylett.9b01308
ACS Energy Lett. 2019, 4, 2168−2180

goal. While it is unlikely that catalysts consisting of biomolecules will serve this purpose, we expect that lessons learned from mimicking biology will enable major steps toward this objective.

H_2O Oxidation. In oxygenic photosynthesis, H_2O oxidation (Table 1) generates O_2 and liberates electrons and protons for generating NADPH and contributing to the transmembrane pH gradient necessary for ATP synthesis.[67] This reaction is remarkable in that it is a light-driven reaction of a selective $4e^-/4H^+$ process. From a broader energy perspective, H_2O oxidation can yield electrons and protons for synthesis of chemical fuels, giving a benign byproduct. In natural photosynthesis, H_2O oxidation is carried out by the oxygen-evolving complex (OEC) of photosystem II (PSII), consisting of a Mn_4CaO_5 cluster.[68] The flow of electrons from H_2O oxidation at the OEC is to the $P680^{+\bullet}$ radical that is generated through electron transfer from a photoexcited state. One of the ways that efficient electron transfer is achieved is through mediators such as the tyrosine (Y_Z) that accepts an electron from the Mn_4CaO_5 cluster (Figure 8). Bioinspired catalysts for H_2O oxidation often incorporate multinuclear centers, electron mediators, and multiple sites for water binding, akin to the OEC in PSII.

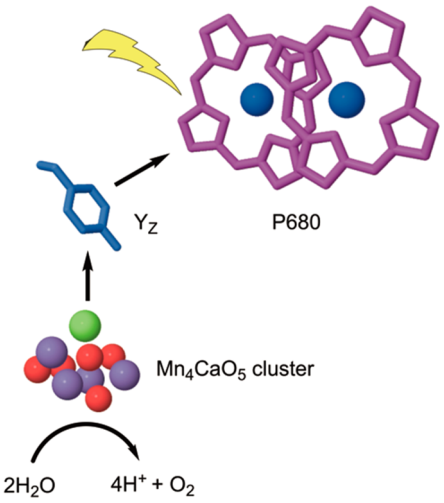

Figure 8. Electron transfer from the Mn_4CaO_5 cluster to P680 mediated by tyrosine (Y_Z). PDB ID: 4UB6.

Engineered Protein Model of Water-Oxidizing OEC. The complexity of the OEC active site structure makes it a challenging target to mimic within a protein environment. A rare successful approach to this problem was demonstrated through the incorporation of a synthetic biotinylated-Co_4O_4 cubane complex (Figure 9a) into streptavidin (Sav) (Figure 9b,c).[69] The biotinylated-Co_4O_4–Sav complexes are able to capture the essential structural elements of the OEC. They exhibit an ordered H-bonding network that connects the Co_4O_4 cluster to the protein, and the asymmetry of the cubane Co_4O_4 complex evokes the asymmetry of the Mn_4CaO_5 cluster that makes H_2O oxidation possible.[70,71] In the variant, biot-*β*-Ala-**1**⊂2xm-Sav, the aqua ligand (O1) of Co1 is H-bonded to a structural water molecule (O3), and that O3 is H-bonded to a serine residue (S112) (Figure 9b). Another variant was made to mimic the Y_Z in PSII by mutating S112 to tyrosine (biot-*β*-Ala-**1**⊂2xm-S_{112}Y-Sav), giving rise to a new H-bonding network where the O1 is directly H-bonded to the Y112

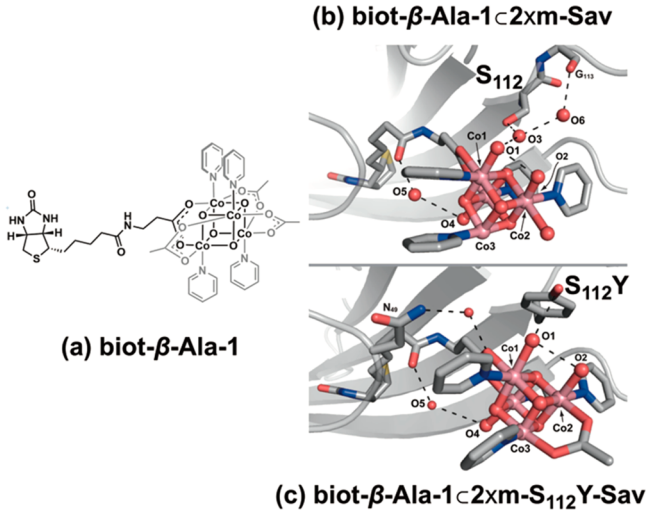

Figure 9. (a) Biotinylated-Co_4O_4 complex (biot-*β*-Ala-1), (b) biot-*β*-Ala-1 incorporated into Sav (PDB ID: 6AUC), and (c) a S112Y mutation in Sav results in direct H-bonding of O1 to the Y112 (PDB ID: 6AUE). Panels a and b are reprinted from ref 69. Copyright 2018 American Chemical Society.

(Figure 9c). This construct is shown to exhibit multiproton/multielectron reactivity. Although it is not a catalyst, it represents an important step toward constructing biomolecular systems modeling the OEC.

Bioinspired Synthetic Catalysts for Water Oxidation. In contrast with biomolecular systems, there are many examples of synthetic models of the OEC. This has been a tempting area for inorganic chemists attracted by the novel inorganic cluster active site.[72] There are synthetic clusters that structurally mimic the Mn_4CaO_5 cluster in the OEC, but catalytic H_2O oxidation activity to yield primarily O_2 from these systems has not been reported yet.[73,74] However, there is progress toward the development of related metal clusters incorporating H-bonding moieties to facilitate proton transfers. For example, a tetranuclear manganese OEC model with H-bonding substituents electrocatalytically forms hydrogen peroxide (H_2O_2) with 15% faradic efficiency (FE).[75] A larger cluster consisting of 12 manganese ions, Mn_{12}DH (Figure 10), electrocatalytically oxidizes H_2O to O_2 at a modest overpotential of 334 mV (using the onset potential) and high (78%) FE.[76] Mn_{12}DH mimics the Mn(IV)–O–Mn(III)–H_2O motif in native OEC, and the hydroxyl groups on the 3,5-dihydroxybenzoic acid ligands of Mn_{12}DH complex enable the catalyst to work in water, while also providing proton shuttles through H-bonding. The efficiency of this catalyst is attributed to the multiple H_2O binding sites in the cluster and the 12 manganese ions that facilitate multielectron redox chemistry.

While many approaches to water oxidation catalysis have utilized multimetallic species inspired by the OEC, others have shown that one redox-active metal may be active for this reaction, in particular when paired with other features inspired by the OEC. For example, a copper complex was designed to possess redox-accessible ligands containing hydroxyl groups to provide a strategy for PCET processes and lower overpotentials for water oxidation.[77] This complex contains a bipyridine ligand with pendant hydroxyl groups meant to mimic Y_Z (Cu-**L**, Figure 11a,b). Electrochemical studies demonstrate H_2O oxidation at modest overpotentials of 510–560 mV (using the half-wave potentials) at pH 12–14

DOI: 10.1021/acsenergylett.9b01308
ACS Energy Lett. 2019, 4, 2168–2180

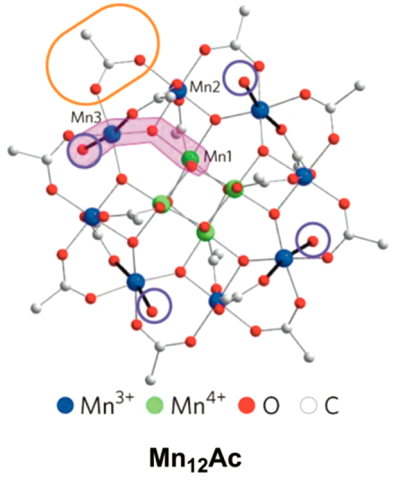

Figure 10. Precursor to Mn_{12}DH, Mn_{12}Ac. Mn_{12}DH was made from treating Mn_{12}Ac with 3,5-dihydroxybenzoic acid. A representative carboxylate is circled in orange, and the water molecules are shown in blue. Reprinted with permission from ref 76. Copyright 2017 Springer Nature.

and O_2 evolution with a FE of 85 ± 5% and a TON of ~400. Attempts to deduce any PCET process with electrocatalysis proved to be difficult, but the authors found that the copper catalyst containing the pendant hydroxyl groups (Cu-**L**) has a 200 mV lower overpotential compared to the copper catalyst without the pendant hydroxyl groups. Another approach has been to pair a redox-inactive metal ion with a redox-active species to mimic the manganese and calcium in the OEC. Investigation of a mononuclear manganese complex associated with a series of redox-inactive ions including Ca^{2+} through an oxo bridge revealed that the Lewis acidity of the redox-inactive ion has significant but divergent influences on electron-transfer, oxygen atom-transfer, and hydrogen atom-transfer reactions, all of which are relevant to water oxidation.[78] These two studies of relatively simple complexes elegantly illustrate successes in drawing on individual components of the intricate structure of the OEC to enhance reactivity of a mononuclear coordination complex toward water oxidation.

Progress and Challenges in Water Oxidation. Recent years have seen improved structural data on PSII as well as details about PSII activity gained through spectroscopy.[79,80] This knowledge provides a crucial guide to biomimetic approaches to water oxidation catalysis. Currently, there are many structural mimics of the OEC, but few that are catalytically active. However, bioinspired complexes incorporating H-bonding interactions and redox-active moieties to direct reactivity have successfully yielded catalysts for the four-electron oxidation of water. Finally, some progress in the construction of biomolecular scaffolds incorporating features of the OEC has been reported recently; this approach provides insight into how biomolecules bind and activate water molecules in a polypeptide environment.

These studies of relatively simple complexes elegantly illustrate successes in drawing on individual components of the intricate structure of the OEC to enhance reactivity of a mononuclear coordination complex toward water oxidation.

Achieving H_2O oxidation selectively to O_2 in biomimetic catalysts remains a tall order. The high potential required for this reaction leads to damage to organic moieties, whether they be synthetic ligands or a protein scaffold. Developing new approaches to avoid or "heal" catalyst damage is particularly important in this area. These efforts may benefit from advances in understanding this process in biology; however, the PSII repair process is complex.[81] While materials-based catalysts for H_2O oxidation suffer less from these problems, and feature self-healing activity in some cases,[82] the pursuit of molecular systems remains a valuable approach to developing our fundamental mechanistic understanding of how nature achieves this remarkable reactivity.

CO_2 Reduction. In biological CO_2 fixation, a variety of carbon molecules are shuttled into different pathways, generating metabolites required by organisms.[83] From a broader energy perspective, sequestering atmospheric CO_2 and efficiently converting it to useful hydrocarbons including fuels is an alternative to burning fossil fuels. CO_2 reduction is challenging because of the thermodynamic barrier to the first $1e^-$ reduction to form the $CO_2^{\bullet-}$ radical anion and the slow kinetics associated with the chemical inertness of CO_2. Another major challenge with CO_2 reduction is achieving product selectivity, as multiple reduced carbon products are possible and H_2 evolution is necessarily a competing reaction. On the other hand, the range of possible products offers

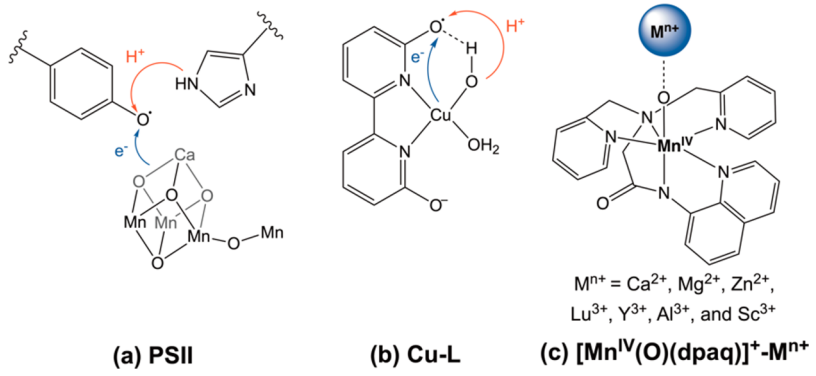

Figure 11. (a) Illustration of PCET process in PSII. (b) Proposed ligand-assisted process in Cu-L. (c) Structure of manganese-oxo complex binding redox-active metal ions.

DOI: 10.1021/acsenergylett.9b01308
ACS Energy Lett. 2019, 4, 2168−2180

opportunities to direct reactivity toward diverse desired outcomes.[84]

Bioinspired complexes and biomolecular catalysts for CO_2 reduction often draw on features of the Ni-containing CO dehydrogenase (Ni-CODH) enzyme, which catalyzes the reversible, proton-coupled reduction of CO_2 to CO.[83] Achieving this transformation can potentially pave the pathway for generating CO for use as a chemical feedstock for more energy-dense, carbon-based fuels. For bioinspired catalytic reduction of CO_2 to more reduced hydrocarbons, there is no enzyme known to perform a multielectron (>2) transformation of CO_2 in nature. However, it has been shown that nitrogenase, which has native activity in catalyzing the $6e^-/6H^+$ reduction of N_2 to NH_3, is also able to reduce CO_2 to hydrocarbons. Finally, the development of catalysts for CO_2 reduction benefits broadly from mimicking strategies used by metalloenzymes to tackle the challenge of directing multiple protons and electrons to achieve catalytic efficiency and product selectivity.

Engineered Protein Catalysts for CO_2 Reduction. Early work on catalysts for CO_2 reduction included the use of nickel- and cobalt-cyclam electrocatalysts (cyclam = 1,4,8,11-tetraazacyclotetradecane) that yield CO.[85] Inspired by the CO_2 reduction activity of the metal-cyclam catalysts, $[Ni(II)\text{-cyclam}]^{2+}$ was coordinated to a solvent-exposed His (H83 or H107) on the copper protein azurin (Figure 12).[86] In addition to conferring water solubility on the catalyst, using azurin also provides a possible electron-transfer site in its native copper, mimicking the function of the iron−sulfur clusters in native Ni-CODH.[83] Azurin variants were made where the $[Ni(II)\text{-cyclam}]^{2+}$ complex is coordinated to one of two surface His residues (H83 or H107; Figure 12).[86] Another set of mutants was made where the copper is replaced with zinc to test the role of a redox-active site for electron transfer. A notable result in electrochemical studies is that copper azurin derivative with $[Ni(II)\text{-cyclam}]^{2+}$ bound to H107 (Figure 12b) displays the lowest overpotential and highest current (reflecting rate) observed in cyclic voltammetry in the presence of CO_2 among these variants. An explanation provided for the enhancement in activity is that the engineered H107 site is more solvent-exposed than H83, enabling the H107-coordinated $[Ni(II)\text{-cyclam}]^{2+}$ to better interact with substrates CO_2 and H^+. Furthermore, the enhanced activity of the Cu derivative is attributed to the role of the Cu site in transferring electrons to the catalyst. In terms of the effects of the native metal site, electrochemical data for the copper variants show higher catalytic currents and increased onset potentials for catalysis (by 130−200 mV, reflecting a lower overpotential and greater efficiency). The TONs with respect to protein catalyst are low (up to ∼37), but this study showcases improvement in selectivity for CO_2 reduction using a protein scaffold and the implications for enhancing catalytic activity through an intramolecular electron transfer between the redox-active copper site and the $[Ni(II)\text{-cyclam}]^{2+}$ complex.

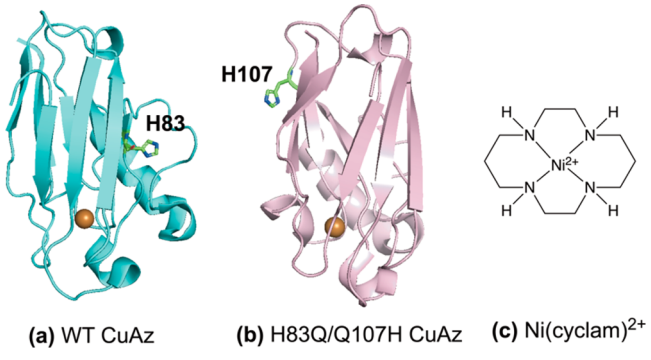

Figure 12. (a) Structure of WT azurin (PDB ID: 4AZU) showing the H83 $[Ni(II)\text{-cyclam}]^{2+}$-binding position. (b) Structure of H83Q/Q107H CuAz (PDB ID: 4AZU) showing the H107 $[Ni(II)\text{-cyclam}]^{2+}$-binding position. (c) Drawing of Ni(II)-cyclam.

Nitrogenases are known to catalyze the reduction of CO_2 to hydrocarbons[87,88] and thus have been developed as biocatalysts for CO_2 reduction.[89] Nitrogenase is a multimetallic enzyme, consisting of the electron-delivery Fe protein and the catalytic protein (FeMo-, V-, or Fe only nitrogenase) that interact through ATP hydrolysis. The catalytic protein contains the P cluster that accepts electrons from the Fe protein and transfers them to the M cluster, which performs N_2-binding and reduction to NH_3.[90] In order to circumvent the energy requirement of ATP hydrolysis for electron donation by the Fe protein, [FeFe]- and [FeMo]-nitrogenases were immobilized onto electrodes with cobaltocene as an electron mediator to provide the electrons to the nitrogenase catalysts.[91] Both [FeFe]- and [FeMo]-nitrogenases were found to produce formate from CO_2 and H_2 from H^+. In Fe protein-ATP driven CO_2 reduction by the nitrogenases, the [FeFe]-nitrogenase

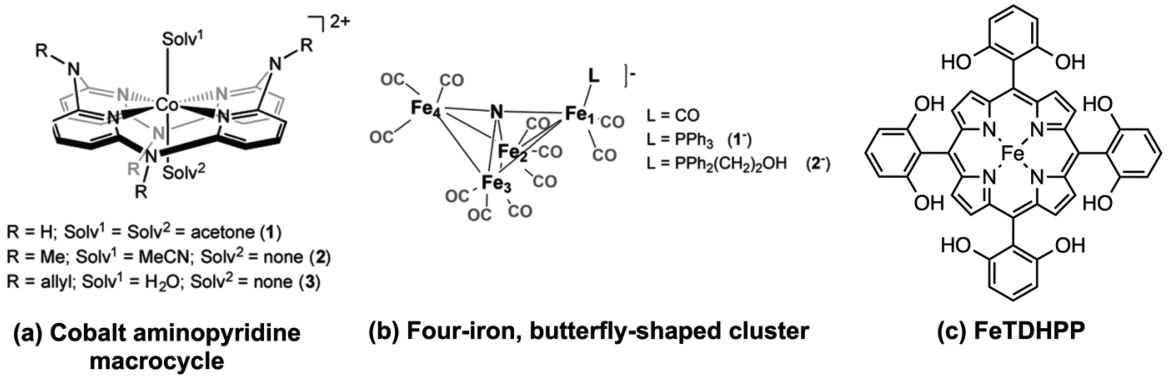

Figure 13. (a) Cobalt aminopyridine macrocycle containing different R substituents on the pendant amine. Complexes 1−3 also feature a solvent molecule coordinated in the axial position. Panel a is reprinted from ref 94. Copyright 2016 American Chemical Society. (b) Four-iron, butterfly-shaped cluster where L contains either the hydroxyl proton relay (2) or just a phosphine ligand (1). Panel b is reprinted with permission from ref 96. Copyright 2016 The Royal Society of Chemistry. (c) Drawing of FeTDHPP.

DOI: 10.1021/acsenergylett.9b01308
ACS Energy Lett. 2019, 4, 2168−2180

produces formate with a FE of 31.0 ± 0.29%, and the [FeMo]-nitrogenase produces formate with a FE of 9.0 ± 1.4%, with the rest of the electrons going toward making H_2. In electrocatalysis, [FeFe]-nitrogenase and [FeMo]-nitrogenase produce formate with a FE of 32.0 ± 1.8% and 8.0 ± 1.6%, respectively. The basis for enhanced CO_2 reduction by [FeFe]-nitrogenase remains to be determined. Few systems catalyze the full $8e^-/8H^+$ reduction of CO_2 to CH_4; thus, further development of this system is of interest.

Bioinspired Synthetic Catalysts for CO_2 Reduction. In CODH, CO_2 binding to the nickel center is stabilized by the interaction of the oxygen atoms with lysine and histidine residues, serving as proton relays and participating in H-bonding networks to assist in substrate activation.[92,93] Modeling these kinds of interactions, a cobalt aminopyridine macrocycle containing amine proton relays (complex **1**, Figure 13a) was developed to catalyze the reduction of CO_2 to CO with a FE of 98 ± 2%, a TON of 1 000 000, and a TOF of 107 s^{-1}.[94] This high activity is attributed to the pendant amines on the ligand backbone that shuttle protons to the active site (Figure 13a). In the derivative where the amine is methylated (complex **2**, Figure 13a), performance is greatly diminished; the FE is 23 ± 2%, TON is 3600, and TOF is 0.5 s^{-1}. In subsequent work, it was demonstrated that the proton-shuttling mechanism relies on the association of acid molecules from solution to the amine groups, reminiscent of how proteins position internal water molecules for proton transfer.[95] Another insight gained through investigation of derivatives of this complex is that the reaction overpotential can be tuned by shifting the Co(I)/Co(0) couple observed in cyclic voltammetry.[94]

Incorporating proton relays into a catalyst for CO_2 reduction may in some cases enhance the competing reaction of H_2 production. For example, the "four-iron, butterfly-shaped" cluster shown in Figure 13b (**1**) selectively reduces CO_2 to formate, also yielding H_2 byproduct.[96] However, installing a proton shuttle (**2**) leads to selective reduction of H^+ to H_2 at high FE.[96,97] The TONs achieved are low (formate TON of 5.4 ± 3 and H_2 TON of 3.3 ± 2 for **1** and H_2 TON of 40 ± 5 for **2**), but this work demonstrates how selectivity for CO_2 vs H^+ reduction may be tuned with proton relays. The examples discussed show striking and contrasting differences in selectivity for CO_2 reduction when a proton relay is involved, but they give insight into ways that proton delivery may be controlled to impact product selectivity.

Iron porphyrin derivatives have proven to be excellent CO_2 reduction catalysts, in particular when proton-shuttling mechanisms are featured. In an iron-tetraphenylporphyrin (FeTPP) complex, installation of hydroxyl groups at the ortho and ortho′ positions (FeTDHPP, Figure 13c) gives rise to an efficient catalyst for CO_2 reduction to CO.[98] FeTDHPP catalyzes CO_2 reduction to CO with a FE of 96% and TON of 50 × 10^6, and the efficiency is attributed to the hydroxyl groups of FeTDHPP providing a local proton source, as determined by comparison to a derivative with methoxy groups in place of the hydroxyl groups (FeTDMPP). FeTDHPP operates at overpotentials of 410−560 mV (based on potentials from foot-of-the-wave-analysis), giving logTOFs of 2.3−4.2, whereas FeTDMPP displays similar logTOFs of 1.3−2.5 but at the cost of much greater overpotentials of 890−1040 mV. In follow-up studies, the authors propose that the hydroxyl groups in the ortho/ortho′ positions provide H-bonding to stabilize the Fe−CO_2 adduct and play a role in PCET to break a C−O bond to generate CO.[99]

Progress and Challenges in CO_2 Reduction. Catalysts for reduction of CO_2 to a single product in the absence of H_2 evolution remain rare. However, the use of protein scaffolds and biomimetic proton relays in synthetic catalysts has yielded promising results in which substrate and product selectivity have been substantially improved. Predicting the effects of H-bonding groups and proton relays on reactivity, however, remains difficult. Furthermore, the preponderance of studies has yielded two-electron reduced products (CO and formate); the development of systems that can selectively produce more reduced products, especially liquid fuels and products with C−C bonds, remains an important and ambitious goal.

This Perspective highlights creative ways in which developing catalysts for energy conversion is approached, using inspiration from natural systems. Metalloenzymes and the ways that they coordinate metal ions and transfer protons provide much of the framework for the design of the complexes and engineered biomolecules discussed. In particular, the introduction of second-sphere interactions, proton-transfer relays, and/or an active-site microenvironment has led to notable improvements in catalyst properties and activity, whether this is through utilizing an existing protein scaffold or building bioinspired features into a synthetic ligand framework. These approaches have yielded successes in (1) conferring water-solubility on catalysts, (2) lowering reaction overpotential (increasing efficiency), (3) increasing catalytic rate, and (4) changing product selectivity. Ultimately, these methods consider the intimate ways in which protons, electrons, and substrates are transferred or activated in nature's catalysts. These considerations guide us toward better design and enable us to better understand the natural world.

While engineered biomolecular and bioinspired catalysts bring promise to the field of sustainable and renewable energy conversion, many broad challenges remain. For one, the engineering and scaling up of viable systems containing robust molecular or biomolecular catalysts for practical use are difficult, as (bio)molecular catalysts tend to be fragile. However, heterogenizing these catalysts and/or incorporating features determined to be important for reactivity into heterogeneous catalysts are approaches to this problem. Using living systems that have in place nature's pathways for protection and regeneration of catalysts is an alternative approach. Assisting these efforts would be analyses of catalyst deactivation and degradation pathways. Finally, more detailed mechanistic studies of engineered biomolecular catalysts and of synthetic molecular catalysts that function in water are needed. These studies will help researchers face future challenges, including enhancing catalyst durability and tuning substrate and product selectivity.

AUTHOR INFORMATION

ORCID

Kara L. Bren: 0000-0002-8082-3634

Notes

The authors declare no competing financial interest.

Biographies

Jennifer M. Le is a Ph.D. candidate in Chemistry at the University of Rochester. She received her B.S. in Chemistry (conc. Biochemistry) from San José State University. Her research interests are electrocatalytic and photocatalytic H_2 generation using peptide- and protein-based catalysts.

DOI: 10.1021/acsenergylett.9b01308
ACS Energy Lett. 2019, 4, 2168−2180

Kara L. Bren is a Professor in the Department of Chemistry at the University of Rochester. She earned her B.A. in Chemistry at Carleton College and her Ph.D. in Chemistry at Caltech with Harry Gray, followed by postdoctoral training at UC Davis with Gerd LaMar. Her group focuses on developing biomolecular catalysts for energy-related reactions.

■ ACKNOWLEDGMENTS

J.M.L.'s research in the Bren lab focuses on hydrogen production catalyzed by synthetic proteins and is supported by the U.S. Department of Energy, Office of Science, Office of Basic Energy Sciences, under Award DE-FG02-09ER16121. K.L.B.'s work on this Perspective was supported by the National Science Foundation Grant CHE-1708256, which supports her research on synthetic metallopeptide catalysts.

■ REFERENCES

(1) Dempsey, J. L.; Winkler, J. R.; Gray, H. B. Proton-Coupled Electron Flow in Protein Redox Machines. *Chem. Rev.* **2010**, *110* (12), 7024−7039.
(2) Hammes-Schiffer, S.; Soudackov, A. V. Proton-Coupled Electron Transfer in Solution, Proteins, and Electrochemistry †. *J. Phys. Chem. B* **2008**, *112* (45), 14108−14123.
(3) Migliore, A.; Polizzi, N. F.; Therien, M. J.; Beratan, D. N. Biochemistry and Theory of Proton-Coupled Electron Transfer. *Chem. Rev.* **2014**, *114* (7), 3381−3465.
(4) Lubitz, W.; Ogata, H.; Rüdiger, O.; Reijerse, E. Hydrogenases. *Chem. Rev.* **2014**, *114* (8), 4081−4148.
(5) Abou Hamdan, A.; Dementin, S.; Liebgott, P.-P.; Gutierrez-Sanz, O.; Richaud, P.; De Lacey, A. L.; Rousset, M.; Bertrand, P.; Cournac, L.; Léger, C. Understanding and Tuning the Catalytic Bias of Hydrogenase. *J. Am. Chem. Soc.* **2012**, *134* (20), 8368−8371.
(6) Peters, J. W.; Schut, G. J.; Boyd, E. S.; Mulder, D. W.; Shepard, E. M.; Broderick, J. B.; King, P. W.; Adams, M. W. W. [FeFe]- and [NiFe]-Hydrogenase Diversity, Mechanism, and Maturation. *Biochim. Biophys. Acta, Mol. Cell Res.* **2015**, *1853* (6), 1350−1369.
(7) Lubitz, W.; Reijerse, E.; van Gastel, M. [NiFe] and [FeFe] Hydrogenases Studied by Advanced Magnetic Resonance Techniques. *Chem. Rev.* **2007**, *107* (10), 4331−4365.
(8) Pandey, K.; Islam, S. T. A.; Happe, T.; Armstrong, F. A. Frequency and Potential Dependence of Reversible Electrocatalytic Hydrogen Interconversion by [FeFe]-Hydrogenases. *Proc. Natl. Acad. Sci. U. S. A.* **2017**, *114* (15), 3843−3848.
(9) Rountree, E. S.; McCarthy, B. D.; Eisenhart, T. T.; Dempsey, J. L. Evaluation of Homogeneous Electrocatalysts by Cyclic Voltammetry. *Inorg. Chem.* **2014**, *53* (19), 9983−10002.
(10) Liebgott, P.-P.; de Lacey, A. L.; Burlat, B.; Cournac, L.; Richaud, P.; Brugna, M.; Fernandez, V. M.; Guigliarelli, B.; Rousset, M.; Léger, C.; et al. Original Design of an Oxygen-Tolerant [NiFe] Hydrogenase: Major Effect of a Valine-to-Cysteine Mutation near the Active Site. *J. Am. Chem. Soc.* **2011**, *133* (4), 986−997.
(11) Radu, V.; Frielingsdorf, S.; Evans, S. D.; Lenz, O.; Jeuken, L. J. C. Enhanced Oxygen-Tolerance of the Full Heterotrimeric Membrane-Bound [NiFe]-Hydrogenase of *Ralstonia eutropha*. *J. Am. Chem. Soc.* **2014**, *136* (24), 8512−8515.
(12) Dutta, A.; Appel, A. M.; Shaw, W. J. Designing Electrochemically Reversible H_2 Oxidation and Production Catalysts. *Nat. Rev. Chem.* **2018**, *2*, 244−252.
(13) Kleingardner, J. G.; Kandemir, B.; Bren, K. L. Hydrogen Evolution from Neutral Water under Aerobic Conditions Catalyzed by Cobalt Microperoxidase-11. *J. Am. Chem. Soc.* **2014**, *136* (1), 4−7.
(14) Verbaro, D.; Hagarman, A.; Kohli, A.; Schweitzer-Stenner, R. Microperoxidase 11: A Model System for Porphyrin Networks and Heme−Protein Interactions. *JBIC, J. Biol. Inorg. Chem.* **2009**, *14*, 1289−1300.
(15) Bhugun, I.; Lexa, D.; Savéant, J.-M. Homogeneous Catalysis of Electrochemical Hydrogen Evolution by Iron(0) Porphyrins. *J. Am. Chem. Soc.* **1996**, *118* (16), 3982−3983.
(16) Beyene, B. B.; Mane, S. B.; Hung, C.-H. Electrochemical Hydrogen Evolution by Cobalt(II) Porphyrins: Effects of Ligand Modification on Catalytic Activity, Efficiency and Overpotential. *J. Electrochem. Soc.* **2018**, *165* (9), H481−H487.
(17) Lee, C. H.; Dogutan, D. K.; Nocera, D. G. Hydrogen Generation by Hangman Metalloporphyrins. *J. Am. Chem. Soc.* **2011**, *133* (23), 8775−8777.
(18) Kandemir, B.; Chakraborty, S.; Guo, Y.; Bren, K. L. Semisynthetic and Biomolecular Hydrogen Evolution Catalysts. *Inorg. Chem.* **2016**, *55* (2), 467−477.
(19) Firpo, V.; Le, J. M.; Pavone, V.; Lombardi, A.; Bren, K. L. Hydrogen Evolution from Water Catalyzed by Cobalt-Mimochrome VI*a, a Synthetic Mini-Protein. *Chem. Sci.* **2018**, *9* (45), 8582−8589.
(20) Sano, Y.; Onoda, A.; Hayashi, T. Photocatalytic Hydrogen Evolution by a Diiron Hydrogenase Model Based on a Peptide Fragment of Cytochrome *c*556 with an Attached Diiron Carbonyl Cluster and an Attached Ruthenium Photosensitizer. *J. Inorg. Biochem.* **2012**, *108*, 159−162.
(21) Dempsey, J. L.; Brunschwig, B. S.; Winkler, J. R.; Gray, H. B. Hydrogen Evolution Catalyzed by Cobaloximes. *Acc. Chem. Res.* **2009**, *42* (12), 1995−2004.
(22) Bacchi, M.; Berggren, G.; Niklas, J.; Veinberg, E.; Mara, M. W.; Shelby, M. L.; Poluektov, O. G.; Chen, L. X.; Tiede, D. M.; Cavazza, C.; Field, M. J.; Fontecave, M.; Artero, V. Cobaloxime-Based Artificial Hydrogenases. *Inorg. Chem.* **2014**, *53* (15), 8071−8082.
(23) Sommer, D. J.; Vaughn, M. D.; Ghirlanda, G. Protein Secondary-Shell Interactions Enhance the Photoinduced Hydrogen Production of Cobalt Protoporphyrin IX. *Chem. Commun.* **2014**, *50* (100), 15852−15855.
(24) Call, A.; Casadevall, C.; Romero-Rivera, A.; Martin-Diaconescu, V.; Sommer, D. J.; Osuna, S.; Ghirlanda, G.; Lloret-Fillol, J. Improved Electro- and Photocatalytic Water Reduction by Confined Cobalt Catalysts in Streptavidin. *ACS Catal.* **2019**, *9* (7), 5837−5846.
(25) Connolly, P.; Espenson, J. H. Cobalt-Catalyzed Evolution of Molecular Hydrogen. *Inorg. Chem.* **1986**, *25* (16), 2684−2688.
(26) Gross, M. A.; Reynal, A.; Durrant, J. R.; Reisner, E. Versatile Photocatalytic Systems for H_2 Generation in Water Based on an Efficient DuBois-Type Nickel Catalyst. *J. Am. Chem. Soc.* **2014**, *136* (1), 356−366.
(27) Wilson, A. D.; Newell, R. H.; McNevin, M. J.; Muckerman, J. T.; Rakowski DuBois, M.; DuBois, D. L. Hydrogen Oxidation and Production Using Nickel-Based Molecular Catalysts with Positioned Proton Relays. *J. Am. Chem. Soc.* **2006**, *128* (1), 358−366.
(28) Yang, J. Y.; Bullock, R. M.; Shaw, W. J.; Twamley, B.; Fraze, K.; DuBois, M. R.; DuBois, D. L. Mechanistic Insights into Catalytic H_2 Oxidation by Ni Complexes Containing a Diphosphine Ligand with a Positioned Amine Base. *J. Am. Chem. Soc.* **2009**, *131* (16), 5935−5945.
(29) Chernev, P.; Lambertz, C.; Brünje, A.; Leidel, N.; Sigfridsson, K. G. V.; Kositzki, R.; Hsieh, C.-H.; Yao, S.; Schiwon, R.; Driess, M.; Limberg, C.; Happe, T.; Haumann, T. Hydride Binding to the Active Site of [FeFe]-Hydrogenase. *Inorg. Chem.* **2014**, *53* (22), 12164−12177.
(30) Knörzer, P.; Silakov, A.; Foster, C. E.; Armstrong, F. A.; Lubitz, W.; Happe, T. Importance of the Protein Framework for Catalytic Activity of [FeFe]-Hydrogenases. *J. Biol. Chem.* **2012**, *287* (2), 1489−1499.
(31) Boralugodage, N. P.; Arachchige, R. J.; Dutta, A.; Buchko, G. W.; Shaw, W. J. Evaluating the Role of Acidic, Basic, and Polar Amino Acids and Dipeptides on a Molecular Electrocatalyst for H_2 Oxidation. *Catal. Sci. Technol.* **2017**, *7* (5), 1108−1121.
(32) Dutta, A.; DuBois, D. L.; Roberts, J. A. S.; Shaw, W. J. Amino Acid Modified Ni Catalyst Exhibits Reversible H_2 Oxidation/Production over a Broad pH Range at Elevated Temperatures. *Proc. Natl. Acad. Sci. U. S. A.* **2014**, *111* (46), 16286−16291.

DOI: 10.1021/acsenergylett.9b01308
ACS Energy Lett. 2019, 4, 2168−2180

(33) Ahmed, M. E.; Dey, S.; Darensbourg, M. Y.; Dey, A. Oxygen-Tolerant H_2 Production by [FeFe]-H_2-ase Active Site Mimics Aided by Second Sphere Proton Shuttle. *J. Am. Chem. Soc.* **2018**, *140* (39), 12457−12468.
(34) Kandemir, B.; Kubie, L.; Guo, Y.; Sheldon, B.; Bren, K. L. Hydrogen Evolution from Water under Aerobic Conditions Catalyzed by a Cobalt ATCUN Metallopeptide. *Inorg. Chem.* **2016**, *55* (4), 1355−1357.
(35) Harford, C.; Sarkar, B. Amino Terminal Cu(II)- and Ni(II)-Binding (ATCUN) Motif of Proteins and Peptides: Metal Binding, DNA Cleavage, and Other Properties. *Acc. Chem. Res.* **1997**, *30* (3), 123−130.
(36) Solis, B. H.; Maher, A. G.; Honda, T.; Powers, D. C.; Nocera, D. G.; Hammes-Schiffer, S. Theoretical Analysis of Cobalt Hangman Porphyrins: Ligand Dearomatization and Mechanistic Implications for Hydrogen Evolution. *ACS Catal.* **2014**, *4* (12), 4516−4526.
(37) Solis, B. H.; Maher, A. G.; Dogutan, D. K.; Nocera, D. G.; Hammes-Schiffer, S. Nickel Phlorin Intermediate Formed by Proton-Coupled Electron Transfer in Hydrogen Evolution Mechanism. *Proc. Natl. Acad. Sci. U. S. A.* **2016**, *113* (3), 485−492.
(38) Bediako, D. K.; Solis, B. H.; Dogutan, D. K.; Roubelakis, M. M.; Maher, A. G.; Lee, C. H.; Chambers, M. B.; Hammes-Schiffer, S.; Nocera, D. G. Role of Pendant Proton Relays and Proton-Coupled Electron Transfer on the Hydrogen Evolution Reaction by Nickel Hangman Porphyrins. *Proc. Natl. Acad. Sci. U. S. A.* **2014**, *111* (42), 15001−15006.
(39) Dempsey, J. L.; Winkler, J. R.; Gray, H. B. Solar Fuels: Approaches to Catalytic Hydrogen Evolution. In *Comprehensive Inorganic Chemistry II*; Elsevier, 2013; pp 553−565. DOI: 10.1016/B978-0-08-097774-4.00806-8.
(40) Galiote, N. A.; de Azevedo, D. C.; Oliveira, O. N.; Huguenin, F. Investigating the Kinetic Mechanisms of the Oxygen Reduction Reaction in a Nonaqueous Solvent. *J. Phys. Chem. C* **2014**, *118* (38), 21995−22002.
(41) Tripkovic, V. Thermodynamic Assessment of the Oxygen Reduction Activity in Aqueous Solutions. *Phys. Chem. Chem. Phys.* **2017**, *19* (43), 29381−29388.
(42) Pegis, M. L.; Wise, C. F.; Martin, D. J.; Mayer, J. M. Oxygen Reduction by Homogeneous Molecular Catalysts and Electrocatalysts. *Chem. Rev.* **2018**, *118* (5), 2340−2391.
(43) Sui, S.; Wang, X.; Zhou, X.; Su, Y.; Riffat, S.; Liu, C. A Comprehensive Review of Pt Electrocatalysts for the Oxygen Reduction Reaction: Nanostructure, Activity, Mechanism and Carbon Support in PEM Fuel Cells. *J. Mater. Chem. A* **2017**, *5* (5), 1808−1825.
(44) Yoshikawa, S.; Muramoto, K.; Shinzawa-Itoh, K. Proton-Pumping Mechanism of Cytochrome c Oxidase. *Annu. Rev. Biophys.* **2011**, *40* (1), 205−223.
(45) Sousa, F. L.; Alves, R. J.; Ribeiro, M. A.; Pereira-Leal, J. B.; Teixeira, M.; Pereira, M. M. The Superfamily of Heme−Copper Oxygen Reductases: Types and Evolutionary Considerations. *Biochim. Biophys. Acta, Bioenerg.* **2012**, *1817* (4), 629−637.
(46) Ferguson-Miller, S.; Babcock, G. T. Heme/Copper Terminal Oxidases. *Chem. Rev.* **1996**, *96* (7), 2889−2908.
(47) Ehudin, M. A.; Schaefer, A. W.; Adam, S. M.; Quist, D. A.; Diaz, D. E.; Tang, J. A.; Solomon, E. I.; Karlin, K. D. Influence of Intramolecular Secondary Sphere Hydrogen-Bonding Interactions on Cytochrome c Oxidase Inspired Low-Spin Heme−Peroxo−Copper Complexes. *Chem. Sci.* **2019**, *10*, 2893−2905.
(48) Nastri, F.; Chino, M.; Maglio, O.; Bhagi-Damodaran, A.; Lu, Y.; Lombardi, A. Design and Engineering of Artificial Oxygen-Activating Metalloenzymes. *Chem. Soc. Rev.* **2016**, *45* (18), 5020−5054.
(49) Sigman, J. A.; Kwok, B. C.; Lu, Y. From Myoglobin to Heme-Copper Oxidase: Design and Engineering of a Cu B Center into Sperm Whale Myoglobin. *J. Am. Chem. Soc.* **2000**, *122* (34), 8192−8196.
(50) Mukherjee, S.; Mukherjee, A.; Bhagi-Damodaran, A.; Mukherjee, M.; Lu, Y.; Dey, A. A Biosynthetic Model of Cytochrome c Oxidase as an Electrocatalyst for Oxygen Reduction. *Nat. Commun.* **2015**, *6* (1), 8467.
(51) Bhagi-Damodaran, A.; Michael, M. A.; Zhu, Q.; Reed, J.; Sandoval, B. A.; Mirts, E. N.; Chakraborty, S.; Moënne-Loccoz, P.; Zhang, Y.; Lu, Y. Why Copper Is Preferred over Iron for Oxygen Activation and Reduction in Haem-Copper Oxidases. *Nat. Chem.* **2017**, *9* (3), 257−263.
(52) Shaanan, B. The Iron−Oxygen Bond in Human Oxyhaemoglobin. *Nature* **1982**, *296* (5858), 683−684.
(53) Hamdane, D.; Zhang, H.; Hollenberg, P. Oxygen Activation by Cytochrome P450 Monooxygenase. *Photosynth. Res.* **2008**, *98* (1−3), 657−666.
(54) Ye, S.; Riplinger, C.; Hansen, A.; Krebs, C.; Bollinger, J. M.; Neese, F. Electronic Structure Analysis of the Oxygen-Activation Mechanism by Fe(II) - and α-Ketoglutarate (AKG)-Dependent Dioxygenases. *Chem. - Eur. J.* **2012**, *18* (21), 6555−6567.
(55) Poulos, T. L. Heme Enzyme Structure and Function. *Chem. Rev.* **2014**, *114* (7), 3919−3962.
(56) Vidakovic, M.; Sligar, S. G.; Li, H.; Poulos, T. L. Understanding the Role of the Essential Asp251 in Cytochrome P450cam Using Site-Directed Mutagenesis, Crystallography, and Kinetic Solvent Isotope Effect. *Biochemistry* **1998**, *37* (26), 9211−9219.
(57) Tian, G.; Berry, J. A.; Klinman, J. P. Oxygen-18 Kinetic Isotope Effects in the Dopamine-Beta-Monooxygenase Reaction: Evidence for a New Chemical Mechanism in Non-Heme, Metallomonooxygenase. *Biochemistry* **1994**, *33* (1), 226−234.
(58) Yamaguchi, S.; Nagatomo, S.; Kitagawa, T.; Funahashi, Y.; Ozawa, T.; Jitsukawa, K.; Masuda, H. Copper Hydroperoxo Species Activated by Hydrogen-Bonding Interaction with Its Distal Oxygen. *Inorg. Chem.* **2003**, *42* (22), 6968−6970.
(59) Mann, S. I.; Heinisch, T.; Ward, T. R.; Borovik, A. S. Peroxide Activation Regulated by Hydrogen Bonds within Artificial Cu Proteins. *J. Am. Chem. Soc.* **2017**, *139* (48), 17289−17292.
(60) Bhunia, S.; Rana, A.; Roy, P.; Martin, D. J.; Pegis, M. L.; Roy, B.; Dey, A. Rational Design of Mononuclear Iron Porphyrins for Facile and Selective 4e-/4H^+ O_2 Reduction: Activation of O−O Bond by 2nd Sphere Hydrogen Bonding. *J. Am. Chem. Soc.* **2018**, *140* (30), 9444−9457.
(61) Gorbikova, E. A.; Belevich, I.; Wikstrom, M.; Verkhovsky, M. I. The Proton Donor for OO Bond Scission by Cytochrome *c* Oxidase. *Proc. Natl. Acad. Sci. U. S. A.* **2008**, *105* (31), 10733−10737.
(62) Proshlyakov, D. A.; Pressler, M. A.; Babcock, G. T. Dioxygen Activation and Bond Cleavage by Mixed-Valence Cytochrome *c* Oxidase. *Proc. Natl. Acad. Sci. U. S. A.* **1998**, *95* (14), 8020−8025.
(63) Schaefer, A. W.; Kieber-Emmons, M. T.; Adam, S. M.; Karlin, K. D.; Solomon, E. I. Phenol-Induced O−O Bond Cleavage in a Low-Spin Heme−Peroxo−Copper Complex: Implications for O_2 Reduction in Heme−Copper Oxidases. *J. Am. Chem. Soc.* **2017**, *139* (23), 7958−7973.
(64) Koutsoupakis, C.; Kolaj-Robin, O.; Soulimane, T.; Varotsis, C. Probing Protonation/Deprotonation of Tyrosine Residues in Cytochrome *ba*3 Oxidase from *Thermus thermophilus* by Time-Resolved Step-Scan Fourier Transform Infrared Spectroscopy. *J. Biol. Chem.* **2011**, *286* (35), 30600−30605.
(65) Shook, R. L.; Peterson, S. M.; Greaves, J.; Moore, C.; Rheingold, A. L.; Borovik, A. S. Catalytic Reduction of Dioxygen to Water with a Monomeric Manganese Complex at Room Temperature. *J. Am. Chem. Soc.* **2011**, *133* (15), 5810−5817.
(66) Schowen, K. B.; Limbach, H.-H.; Denisov, G. S.; Schowen, R. L. Hydrogen Bonds and Proton Transfer in General-Catalytic Transition-State Stabilization in Enzyme Catalysis. *Biochim. Biophys. Acta, Bioenerg.* **2000**, *1458* (1), 43−62.
(67) Nelson, N.; Ben-Shem, A. Correction: The Complex Architecture of Oxygenic Photosynthesis. *Nat. Rev. Mol. Cell Biol.* **2004**, *5* (12), 971−982.
(68) Kawakami, K.; Umena, Y.; Kamiya, N.; Shen, J.-R. Structure of the Catalytic, Inorganic Core of Oxygen-Evolving Photosystem II at 1.9Å Resolution. *J. Photochem. Photobiol., B* **2011**, *104* (1−2), 9−18.

DOI: 10.1021/acsenergylett.9b01308
ACS Energy Lett. 2019, 4, 2168−2180

(69) Olshansky, L.; Huerta-Lavorie, R.; Nguyen, A. I.; Vallapurackal, J.; Furst, A.; Tilley, T. D.; Borovik, A. S. Artificial Metalloproteins Containing Co_4O_4 Cubane Active Sites. *J. Am. Chem. Soc.* **2018**, *140* (8), 2739−2742.
(70) Kanan, M. W.; Yano, J.; Surendranath, Y.; Dincă, M.; Yachandra, V. K.; Nocera, D. G. Structure and Valency of a Cobalt-Phosphate Water Oxidation Catalyst Determined by in Situ X-Ray Spectroscopy. *J. Am. Chem. Soc.* **2010**, *132* (39), 13692−13701.
(71) Pushkar, Y.; Yano, J.; Sauer, K.; Boussac, A.; Yachandra, V. K. Structural Changes in the Mn4Ca Cluster and the Mechanism of Photosynthetic Water Splitting. *Proc. Natl. Acad. Sci. U. S. A.* **2008**, *105* (6), 1879−1884.
(72) Blakemore, J. D.; Crabtree, R. H.; Brudvig, G. W. Molecular Catalysts for Water Oxidation. *Chem. Rev.* **2015**, *115* (23), 12974−13005.
(73) Manchanda, R.; Brudvig, G. W.; Crabtree, R. H. High-Valent Oxomanganese Clusters: Structural and Mechanistic Work Relevant to the Oxygen-Evolving Center in Photosystem II. *Coord. Chem. Rev.* **1995**, *144*, 1−38.
(74) Paul, S.; Neese, F.; Pantazis, D. A. Structural Models of the Biological Oxygen-Evolving Complex: Achievements, Insights, and Challenges for Biomimicry. *Green Chem.* **2017**, *19* (10), 2309−2325.
(75) Han, Z.; Horak, K. T.; Lee, H. B.; Agapie, T. Tetranuclear Manganese Models of the OEC Displaying Hydrogen Bonding Interactions: Application to Electrocatalytic Water Oxidation to Hydrogen Peroxide. *J. Am. Chem. Soc.* **2017**, *139* (27), 9108−9111.
(76) Maayan, G.; Gluz, N.; Christou, G. A Bioinspired Soluble Manganese Cluster as a Water Oxidation Electrocatalyst with Low Overpotential. *Nat. Catal.* **2018**, *1* (1), 48−54.
(77) Zhang, T.; Wang, C.; Liu, S.; Wang, J.-L.; Lin, W. A Biomimetic Copper Water Oxidation Catalyst with Low Overpotential. *J. Am. Chem. Soc.* **2014**, *136* (1), 273−281.
(78) Sankaralingam, M.; Lee, Y.-M.; Pineda-Galvan, Y.; Karmalkar, D. G.; Seo, M. S.; Jeon, S. H.; Pushkar, Y.; Fukuzumi, S.; Nam, W. Redox Reactivity of a Mononuclear Manganese-Oxo Complex Binding Calcium Ion and Other Redox-Inactive Metal Ions. *J. Am. Chem. Soc.* **2019**, *141* (3), 1324−1336.
(79) Suga, M.; Akita, F.; Hirata, K.; Ueno, G.; Murakami, H.; Nakajima, Y.; Shimizu, T.; Yamashita, K.; Yamamoto, M.; Ago, H.; Shen, J.-R. Native Structure of Photosystem II at 1.95 Å Resolution Viewed by Femtosecond X-Ray Pulses. *Nature* **2015**, *517* (7532), 99−103.
(80) Oyala, P. H.; Stich, T. A.; Debus, R. J.; Britt, R. D. Ammonia Binds to the Dangler Manganese of the Photosystem II Oxygen-Evolving Complex. *J. Am. Chem. Soc.* **2015**, *137* (27), 8829−8837.
(81) Järvi, S.; Suorsa, M.; Aro, E.-M. Photosystem II Repair in Plant Chloroplasts — Regulation, Assisting Proteins and Shared Components with Photosystem II Biogenesis. *Biochim. Biophys. Acta, Bioenerg.* **2015**, *1847* (9), 900−909.
(82) Najafpour, M. M.; Fekete, M.; Sedigh, D. J.; Aro, E.-M.; Carpentier, R.; Eaton-Rye, J. J.; Nishihara, H.; Shen, J.-R.; Allakhverdiev, S. I.; Spiccia, L. Damage Management in Water-Oxidizing Catalysts: From Photosystem II to Nanosized Metal Oxides. *ACS Catal.* **2015**, *5* (3), 1499−1512.
(83) Can, M.; Armstrong, F. A.; Ragsdale, S. W. Structure, Function, and Mechanism of the Nickel Metalloenzymes, CO Dehydrogenase, and Acetyl-CoA Synthase. *Chem. Rev.* **2014**, *114* (8), 4149−4174.
(84) Appel, A. M.; Bercaw, J. E.; Bocarsly, A. B.; Dobbek, H.; DuBois, D. L.; Dupuis, M.; Ferry, J. G.; Fujita, E.; Hille, R.; Kenis, P. J. A.; et al. Frontiers, Opportunities, and Challenges in Biochemical and Chemical Catalysis of CO_2 Fixation. *Chem. Rev.* **2013**, *113* (8), 6621−6658.
(85) Fisher, B. J.; Eisenberg, R. Electrocatalytic Reduction of Carbon Dioxide by Using Macrocycles of Nickel and Cobalt. *J. Am. Chem. Soc.* **1980**, *102* (24), 7361−7363.
(86) Schneider, C. R.; Shafaat, H. S. An Internal Electron Reservoir Enhances Catalytic CO_2 Reduction by a Semisynthetic Enzyme. *Chem. Commun.* **2016**, *52* (64), 9889−9892.
(87) Seefeldt, L. C.; Rasche, M. E.; Ensign, S. A. Carbonyl Sulfide and Carbon Dioxide as New Substrates, and Carbon Disulfide as a New Inhibitor, of Nitrogenase. *Biochemistry* **1995**, *34* (16), 5382−5389.
(88) Lee, C. C.; Hu, Y.; Ribbe, M. W. Vanadium Nitrogenase Reduces CO. *Science (Washington, DC, U. S.)* **2010**, *329* (5992), 642−642.
(89) Seefeldt, L. C.; Yang, Z.-Y.; Duval, S.; Dean, D. R. Nitrogenase Reduction of Carbon-Containing Compounds. *Biochim. Biophys. Acta, Bioenerg.* **2013**, *1827* (8−9), 1102−1111.
(90) Hoffman, B. M.; Lukoyanov, D.; Dean, D. R.; Seefeldt, L. C. Nitrogenase: A Draft Mechanism. *Acc. Chem. Res.* **2013**, *46* (2), 587−595.
(91) Hu, B.; Harris, D. F.; Dean, D. R.; Liu, T. L.; Yang, Z.-Y.; Seefeldt, L. C. Electrocatalytic CO2 Reduction Catalyzed by Nitrogenase MoFe and FeFe Proteins. *Bioelectrochemistry* **2018**, *120*, 104−109.
(92) Yadav, R. K.; Baeg, J.-O.; Oh, G. H.; Park, N.-J.; Kong, K.; Kim, J.; Hwang, D. W.; Biswas, S. K. A Photocatalyst−Enzyme Coupled Artificial Photosynthesis System for Solar Energy in Production of Formic Acid from CO_2. *J. Am. Chem. Soc.* **2012**, *134* (28), 11455−11461.
(93) Gong, W.; Hao, B.; Wei, Z.; Ferguson, D. J.; Tallant, T.; Krzycki, J. A.; Chan, M. K. Structure of the Ni-Dependent CO Dehydrogenase Component of the Methanosarcina Barkeri Acetyl-CoA Decarbonylase/Synthase Complex. *Proc. Natl. Acad. Sci. U. S. A.* **2008**, *105* (28), 9558−9563.
(94) Chapovetsky, A.; Do, T. H.; Haiges, R.; Takase, M. K.; Marinescu, S. C. Proton-Assisted Reduction of CO_2 by Cobalt Aminopyridine Macrocycles. *J. Am. Chem. Soc.* **2016**, *138* (18), 5765−5768.
(95) Chapovetsky, A.; Welborn, M.; Luna, J. M.; Haiges, R.; Miller, T. F.; Marinescu, S. C. Pendant Hydrogen-Bond Donors in Cobalt Catalysts Independently Enhance CO_2 Reduction. *ACS Cent. Sci.* **2018**, *4* (3), 397−404.
(96) Loewen, N. D.; Thompson, E. J.; Kagan, M.; Banales, C. L.; Myers, T. W.; Fettinger, J. C.; Berben, L. A. A Pendant Proton Shuttle on $[Fe_4N(CO)_{12}]$ - Alters Product Selectivity in Formate vs. H_2 Production via the Hydride $[H- Fe_4N(CO)_{12}]$ -. *Chem. Sci.* **2016**, *7* (4), 2728−2735.
(97) Taheri, A.; Thompson, E. J.; Fettinger, J. C.; Berben, L. A. An Iron Electrocatalyst for Selective Reduction of CO_2 to Formate in Water: Including Thermochemical Insights. *ACS Catal.* **2015**, *5* (12), 7140−7151.
(98) Costentin, C.; Drouet, S.; Robert, M.; Savéant, J.-M. A Local Proton Source Enhances CO_2 Electroreduction to CO by a Molecular Fe Catalyst. *Science* **2012**, *338* (6103), 90−94.
(99) Costentin, C.; Passard, G.; Robert, M.; Savéant, J.-M. Pendant Acid−Base Groups in Molecular Catalysts: H-Bond Promoters or Proton Relays? Mechanisms of the Conversion of CO_2 to CO by Electrogenerated Iron(0)Porphyrins Bearing Prepositioned Phenol Functionalities. *J. Am. Chem. Soc.* **2014**, *136* (33), 11821−11829.

DOI: 10.1021/acsenergylett.9b01308
ACS Energy Lett. 2019, 4, 2168−2180